

# PCCP

Physical Chemistry Chemical Physics

Accepted Manuscript

This article can be cited before page numbers have been issued, to do this please use: J. M. Arroyave and M. Avena, *Phys. Chem. Chem. Phys.*, 2020, DOI: 10.1039/D0CP00993H.



This is an Accepted Manuscript, which has been through the Royal Society of Chemistry peer review process and has been accepted for publication.

Accepted Manuscripts are published online shortly after acceptance, before technical editing, formatting and proof reading. Using this free service, authors can make their results available to the community, in citable form, before we publish the edited article. We will replace this Accepted Manuscript with the edited and formatted Advance Article as soon as it is available.

You can find more information about Accepted Manuscripts in the [Information for Authors](#).

Please note that technical editing may introduce minor changes to the text and/or graphics, which may alter content. The journal's standard [Terms & Conditions](#) and the [Ethical guidelines](#) still apply. In no event shall the Royal Society of Chemistry be held responsible for any errors or omissions in this Accepted Manuscript or any consequences arising from the use of any information it contains.

1 **Determining rate coefficients for ion adsorption at the solid/water interface,** View Article Online  
DOI: 10.1039/D0CP00993H

2 **Better from desorption rate than from adsorption rate**

3  
4 Jeison Manuel Arroyave and Marcelo Avena\*

5 INQUISUR, Departamento de Química, Universidad Nacional del Sur (UNS)-  
6 CONICET, Av. Alem 1253, 8000 Bahía Blanca, Argentina

7  
8  
9  
10  
11 **\*Corresponding autor:** Marcelo Avena. INQUISUR, Departamento de Química,  
12 Universidad Nacional del Sur (UNS)-CONICET, Av. Alem 1253, 8000 Bahía Blanca,  
13 Argentina.

14 **E-mail address:** mavena@uns.edu.ar

1 **Abstract**View Article Online  
DOI: 10.1039/D0CP00993H

2 One of the most common approaches in the adsorption kinetic literature is to compare the  
3 fitting performance of several empirical or non-empirical equations (pseudo-first order,  
4 pseudo-second order, Elovich, parabolic diffusion, etc.) with the aim of selecting the  
5 equation that best describes the experimental data. This is normally a futile fitting exercise  
6 that leads to the determination of ambiguous rate parameters, without providing insights  
7 into the behaviour of the studied system. A more realistic approach is to treat it as a  
8 combination of mass transport and chemical reaction under controlled conditions, and  
9 thus actual adsorption-desorption rate parameters are readily estimated. This article  
10 applies a simple and realistic physicochemical model to describe and understand the  
11 adsorption-desorption kinetics of ions at the solid/water interface. The model is applied  
12 to an ATR-FTIR study of phosphate adsorption-desorption on goethite, which is a very  
13 well-known and reference system, ideal for testing the performance of a physicochemical  
14 treatment that combines transport and reaction. Always the same phosphate species  
15 (monodentate mononuclear protonated) was present at the goethite surface during  
16 adsorption-desorption. There was an excellent agreement between theory and  
17 experiments at a variety of phosphate concentration and surface coverages for adsorption  
18 kinetics, desorption kinetics and equilibrium situations, employing just one set of rate  
19 coefficients. The use of rate vs adsorption curves permitted easily to detect conditions of  
20 transport- and reaction-controlled kinetics. The phosphate-goethite system is a fast-  
21 adsorbing/slow-desorbing system, with an adsorption rate constant  $k_a^0=1.26\times 10^3\text{ s}^{-1}$  and a  
22 desorption rate constant  $k_d=1.66\times 10^{-5}\text{ s}^{-1}$ . Therefore, adsorption was transport-controlled  
23 and desorption was reaction-controlled. The half-life of the desorption reaction is 41700  
24 s (11.6 h) but for adsorption it would take only a few seconds in absence of transport  
25 control. For this kind of systems, which are ubiquitous in nature and technological

- 1 processes, it is easier to determine rate constants from desorption than from adsorption
- 2 experiments.
- 3 **Key Words:** adsorption kinetics; oxide-water interface; surface complexes; phosphate
- 4 desorption.

View Article Online  
DOI: 10.1039/D0CP00993H

## 1 **Introduction**

View Article Online  
DOI: 10.1039/D0CP00993H

2 Many environmental and technological processes are governed or influenced by  
3 adsorption-desorption reactions at the solid-water interface. Situations under equilibrium  
4 are usually described by several adsorption models, with rather simple equations, such as  
5 the Langmuir isotherm (1),(2), or with more complicated combinations of equations, such  
6 as surface complexation models (3),(4), that describe adsorption of ions and complexing  
7 molecules at charged solid/liquid interfaces. Dynamic situations, where the kinetics of  
8 adsorption and desorption needs to be modelled, are usually more difficult to undertake,  
9 and thus they are less investigated with proper detail, even though adsorption kinetics is  
10 of paramount significance in environment and technology.

11 In general, the adsorption process from a homogenised or well-stirred bulk  
12 solution results in a combination of mass transport, where the adsorbing species is  
13 transported to the surface, and a chemical (or physical) reaction, where the species that  
14 arrived to the surface by transport establishes the chemical (or physical) bond with surface  
15 groups. Simple kinetic equations or models do not consider the combination of mass  
16 transport and reaction, neglecting one of them when treating adsorption  
17 kinetics(1),(2),(5). This simplified treatment leads to the determination of ambiguous rate  
18 parameters from data fitting because they include the effects of the neglected process. As  
19 a result, the so-obtained parameters can only be applied to conditions that exactly match  
20 the measuring conditions and cannot be safely translated and used in a different situation.

21 One of the most common approaches in the adsorption kinetic literature is to  
22 compare the fitting performance of several empirical or non-empirical equations (pseudo-  
23 first order, pseudo-second order, Elovich, parabolic diffusion, etc.) with the aim of  
24 selecting the equation that best describes the experimental data and obtaining the rate  
25 constant or other parameters that appear in it. As indicated above, the obtained rate

1 constants or parameters are ambiguous, with low physical significance, or even  
2 meaningless. Thus, a whole adsorption desorption kinetic study may become just a fitting  
3 exercise, without providing insights into the behaviour of the studied system, obstructing  
4 our understanding of the mechanisms that govern adsorption-desorption at the solid/liquid  
5 interfaces (6).

6 In spite of the alleged difficulties of kinetic treatments for adsorption-desorption  
7 reactions, there are systems where the dynamics can be undertaken, in principle, without  
8 complications. This is the case of flow systems with ATR-FTIR detection of the adsorbed  
9 species (7). On one side, the flow system allows flowing always fresh solution with a  
10 constant and well controlled adsorbate concentration. On the other side, infrared  
11 spectroscopy can selectively detect the adsorbed species and monitor the change of its  
12 concentration during a kinetic run, allowing for a precise identification and quantification  
13 of the product of the adsorption reaction (8),(9). With the right treatment of the system  
14 and the obtained data, it is possible to identify the conditions where mass transport  
15 controls the kinetics, or where reaction controls it, allowing for a proper evaluation of the  
16 rate parameters, such as the attachment rate constant,  $k_a$ , or the detachment rate constant,  
17  $k_d$  (see below).

18 The overwhelming majority of adsorption-desorption studies rely on adsorption  
19 kinetic data to find the rate parameters (10). Only very few studies used desorption kinetic  
20 information for that purpose (11). Since any adsorption system is a dynamic system,  
21 adsorption always occurs simultaneously with desorption, and what is actually measured  
22 is the net rate of the process. Therefore, the rate parameters can, in principle, be obtained  
23 from adsorption kinetic runs, desorption kinetic runs or both. In addition, as mass  
24 transport is always connected to reaction, there may be situations where transport affects  
25 considerably the adsorption rate, not influencing the desorption rate. Under these

1 conditions, measuring desorption kinetics would be much more useful than measuring  
2 adsorption kinetics. View Article Online  
DOI: 10.1039/D0CP00993H

3       The aim of this paper is to use a very simple but realistic physicochemical model  
4 that combines mass transport and reaction at the surface to describe simultaneously  
5 adsorption and desorption kinetics at the solid/water interface as measured in an ATR-  
6 FTIR flow cell. The treatment is applied to the adsorption-desorption kinetics of  
7 phosphate on goethite in aqueous media. Due to its environmental importance, the system  
8 phosphate-goethite has become a model system and there is abundant information about  
9 adsorption-desorption under very different conditions (3)(9)(12)(13)(14). Such a highly  
10 studied system is ideal to test this simple treatment, and to check whether adsorption  
11 kinetic or desorption kinetic runs are better for determining the rate parameters.

## 12       **Experimental**

13       **Chemicals.** All chemicals were of analytical grade and used as received. Double distilled  
14 water was used for the preparation of solutions.  
15

16       **Synthesis and characterization of goethite.** The goethite used in this study was an  
17 aliquot of a previously prepared and investigated sample (15). It was prepared following  
18 a procedure similar to that described by Atkinson et al. (16). A 5M NaOH solution was  
19 added dropwise to a 0.1 M  $\text{Fe}(\text{NO}_3)_3 \cdot 9\text{H}_2\text{O}$  solution until the final pH was 12. This  
20 reaction led to the formation of a ferrihydrite dispersion, which was then aged at 60°C  
21 during 3 days in a capped teflon bottle, in order to produce goethite crystallization. The  
22 obtained goethite particles were filtered and washed with  $\text{CO}_2$ -free water until the  
23 conductivity of the supernatant was lower than  $10 \mu\text{S cm}^{-1}$ . The washed solid was stored  
24 as a stock suspension ( $9.63 \text{ gL}^{-1}$ ) at pH 4.5 in water. Its  $\text{N}_2$ -BET surface area was 89.7  
25

1  $\text{m}^2\text{g}^{-1}$  and its isoelectric point (IEP) was 8.6. The X-ray diffraction pattern and IR  
2 spectrum were typical of pure goethite. View Article Online  
DOI: 10.1039/D0CP00993H

3

4 **Adsorption isotherm.** An adsorption isotherm at pH 7.0 was obtained by batch  
5 equilibration using 15-mL polypropylene centrifuge tubes, using 0.1M NaCl as  
6 supporting electrolyte. Each tube contained 0.7 mL of the stock goethite suspension and  
7 10 mL of a phosphate solution of known concentration. The tubes were then shaken for  
8 6 h (enough to achieve equilibration) with an end-over-end rotator and then the  
9 concentration of phosphate remaining in the supernatant solution was quantified.

10 Adsorbed phosphate was calculated from the difference between the initial and final  
11 concentrations. Quantification of phosphate in solution was done by UV–VIS  
12 spectrophotometry using the molybdenum blue method (17), recording the spectra in the  
13 200–1000 nm wavelength range and using the absorbance at 880 nm for calculation.  
14 Calibration curves were constructed with phosphate solutions prepared at pH 7.0 in 0.1  
15 M NaCl. An Agilent 8453 UV-Vis diode array spectrophotometer equipped with a 1-cm  
16 Hellma quartz cell was used for spectral readings.

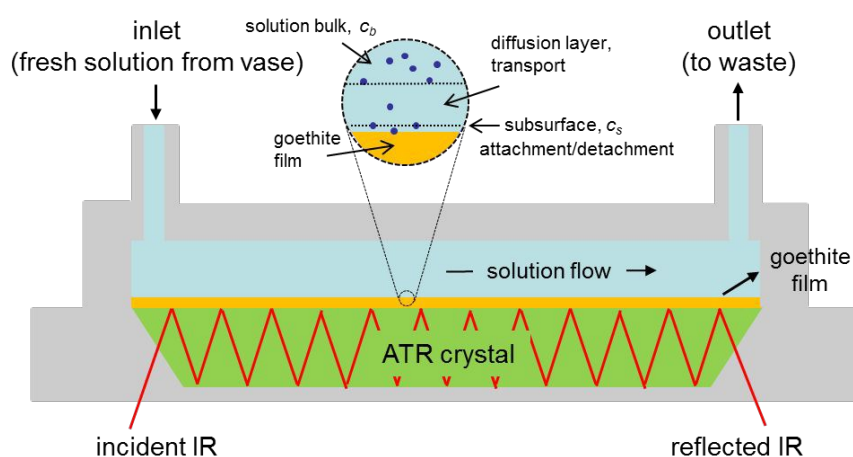
17

18 **ATR-FTIR adsorption-desorption kinetics.** Phosphate adsorption-desorption kinetics  
19 was monitored by ATR-FTIR spectroscopy using a Thermo Fisher Scientific ARK flow  
20 cell containing a ZnSe crystal (area: 10 x 72 mm, incident angle: 45°, total reflections: 12)  
21 as internal reflection element. A schematic representation of the flow cell used for the  
22 measurements is shown in Fig. 1. The goethite film was made by pouring 210  $\mu\text{L}$  of the  
23 stock goethite dispersion over the ZnSe crystal and letting it dry on air. Once the film was  
24 formed, the solution of interest was flown from a reservoir (capped vase with a stirred  
25 solution of controlled pH and temperature, under nitrogen bubbling) to the cell with a



1 Gilson Minipuls 8 peristaltic pump at a flow rate of  $3.3 \text{ mL min}^{-1}$ . An open flow system  
2 was used in all cases, with fresh solution always flowing through the cell, being discarded  
3 by the outlet tubing. The supporting electrolyte was  $0.1 \text{ M NaCl}$  at  $\text{pH } 7.0$  in all cases, and  
4 the working temperature was  $24 \pm 2 \text{ }^\circ\text{C}$ . Each recorded spectrum was the average of 128  
5 scans, with a spectral resolution of  $16 \text{ cm}^{-1}$ .

6



7

8 Fig. 1. Scheme of the flow cell used in the experiments.

9

10 A typical phosphate adsorption-desorption experiment started by flowing the  
11 supporting electrolyte through the cell followed by the acquisition of a blank spectrum.  
12 After that, a phosphate solution of the desired concentration ( $\text{pH } 7.0$ , in  $0.1 \text{ M NaCl}$ ) was  
13 flown to produce phosphate adsorption on goethite, registering IR spectra as a function  
14 of time until the intensity of the signal levelled off (around 3 h for the lowest phosphate  
15 concentration,  $3 \times 10^{-6} \text{ M}$ , and around 1 h for the highest phosphate concentration,  $3 \times 10^{-4}$   
16 M). Once the last spectrum was acquired, the supporting electrolyte was again flown, in  
17 order to induce desorption at the same  $\text{pH}$ , and IR spectra were registered as a function  
18 of time to monitor the desorption kinetics during 1 h. Longer desorption times did not  
19 ensure a stable baseline. A fresh goethite film was prepared for each adsorption-  
20 desorption run. Calibration of the equipment was performed with the aid of the adsorption

1 isotherm under the same working conditions, matching the absorbance at long reaction  
2 times with the adsorbed amount obtained from the isotherm.

3

#### 4 **Theoretical background**

5 The adsorption-desorption kinetics at the solid/liquid interface results from the  
6 combination of transport and attachment-detachment of the reacting ions or molecules.

7 For practical purposes, it is convenient to express the concentration,  $c'$ , as a dimensionless  
8 [-] quantity, dividing the actual molar concentration,  $c$ , by its standard state,  $c^o = 1\text{M}$ .

9 Therefore,  $c' = c/c^o$  and thus, for calculations,  $c'$  has the same magnitude than the molar  
10 concentration but no units. This procedure allows to have rate parameters with proper  
11 units. Therefore, the transport rate,  $J_t$  [ $\text{s}^{-1}$ ], can be expressed as a function of the  
12 concentration gradient in the diffusion layer near the surface (Fig. 1) as follows

$$13 \quad J_t = k_t(c'_b - c'_s) \quad (1)$$

14 Where  $k_t$  [ $\text{s}^{-1}$ ] is a transport rate coefficient,  $c'_b$ , is the concentration of the adsorbing  
15 species in the bulk solution and  $c'_s$  is its concentration on a subsurface layer, adjacent to  
16 the surface. Once located in the subsurface layer, the adsorbing species is already  
17 “touching” the surface, and it just needs to become bonded or attached to the surface  
18 groups. Thus, the species will attach the surface with an attachment rate coefficient  $k_a$   
19 [ $\text{s}^{-1}$ ] and will detach from the surface with a detachment rate coefficient  $k_d$  [ $\text{s}^{-1}$ ], resulting  
20 in an attachment/detachment (reaction) rate,  $\frac{d\theta}{dt}$  [ $\text{s}^{-1}$ ], that is given by forward and  
21 backward terms as follows:

$$22 \quad \frac{d\theta}{dt} = k_a c'_s (1 - \theta) - k_d \theta \quad (2)$$

1 Where  $\theta$  is the surface coverage,  $\theta = \frac{\Gamma}{\Gamma_m}$ ,  $\Gamma$  [ $\mu\text{mol m}^{-2}$ ] is the adsorbed amount per unit  
 2 area and  $\Gamma_m$  [ $\mu\text{mol m}^{-2}$ ] its maximum value, obtained at surface saturation. The rate in  
 3 terms of adsorbed amount,  $\frac{d\Gamma}{dt}$  [ $\mu\text{mol m}^{-2} \text{s}^{-1}$ ], can be easily obtained from

$$4 \quad \frac{d\Gamma}{dt} = \frac{d\theta}{dt} \Gamma_m \quad (3)$$

5 In a steady-state situation the transport rate should equal the reaction rate and thus  
 6 the following expression for  $c'_s$  can be found from the combination of Eq. 1 and 2:

$$7 \quad c'_s = \frac{k_d\theta + k_t c'_b}{k_a(1-\theta) + k_t} \quad (4)$$

8 This expression can be substituted in Eq. 2 to give the general adsorption-  
 9 desorption equation where transport and attachment/detachment are combined

$$10 \quad \frac{d\theta}{dt} = \frac{k_t k_a (1-\theta) c'_b - k_t k_d \theta}{k_a (1-\theta) + k_t} \quad (5)$$

11 This Eq. can be evaluated under equilibrium conditions. Knowing that at  
 12 equilibrium  $\frac{d\theta}{dt} = 0$  and  $c'_b = c'_{eq}$ , where  $c'_{eq}$  is the equilibrium concentration, Eq. 5 leads to:

$$13 \quad \frac{\theta}{(1-\theta)} = \frac{k_a}{k_d} c'_{eq} \quad (6)$$

14 Which is the adsorption isotherm, relating  $\theta$  with  $c'_{eq}$ .

15 Using the adsorption isotherm, and substituting  $k_d\theta$  in Eq. 5 by  $k_a(1-\theta)c'_{eq}$ ,  
 16 another form of eq. 5 is obtained:

$$17 \quad \frac{d\theta}{dt} = \frac{k_t k_a (1-\theta)}{k_a (1-\theta) + k_t} (c'_b - c'_{eq}) \quad (7)$$

18 Where  $c'_{eq}$  corresponds to the  $\theta$  specified in the equation. Equations 5 and 7 are equivalent  
 19 and can be used indistinctively. They represent the general equation that combines  
 20 transport and reaction for calculation of the adsorption-desorption rate at a given  $c'_b$ ,  
 21 provided the values or expressions for  $k_t$ ,  $k_a$ ,  $k_d$  and  $\Gamma_m$  are known. If, for example,  $c'_b >$   
 22  $c'_{eq}$ , the rate is positive ( $\frac{d\theta}{dt} > 0$ ) and thus net adsorption takes place and  $k_t$ ,  $k_a$ ,  $k_d$  can be

1 obtained from an adsorption kinetic run. On the contrary, if  $c'_b < c'_{eq}$  the rate is negative  
 2 ( $\frac{d\theta}{dt} < 0$ ) and thus net desorption takes place and  $k_t, k_a, k_d$  can be obtained from a desorption  
 3 kinetic run. Different special situations can be deduced starting from the general equations  
 4 5 and 7, such as those found under the conditions of transport control, reaction control,  
 5 initial adsorption rate  $\left(\frac{d\theta}{dt}\right)_{i,ads}$ , initial desorption rate  $\left(\frac{d\theta}{dt}\right)_{i,des}$ , etc. These different  
 6 situations and their corresponding equations are listed in Table 1.

7  
 8 **Table 1. Equations of the model used in calculations\***

Condition	General equation	Initial adsorption ( $\Gamma=0, c'_{eq}=0$ )	Initial desorption ( $\Gamma=\Gamma_i, c'_b=0$ )
mixed transport and reaction	$\frac{d\theta}{dt} = \frac{k_t k_a (1-\theta) c'_b - k_t k_d \theta}{k_a (1-\theta) + k_t}$ (5)	$\left(\frac{d\theta}{dt}\right)_{i,ads} = \frac{k_t k_a}{k_a + k_t} c'_b$ (10)	$\left(\frac{d\theta}{dt}\right)_{i,d} = -\frac{k_t k_d \theta_i}{k_a (1-\theta_i) + k_t}$ (13)
	$\frac{d\theta}{dt} = \frac{k_t k_a (1-\theta)}{k_a (1-\theta) + k_t} (c'_b - c'_{eq})$ (7)		
transport control ( $k_a (1-\theta) \gg k_t$ )	$k_a \frac{d\theta}{dt} = k_t (c'_b - c'_{eq})$ (8)	$\left(\frac{d\theta}{dt}\right)_{i,ads} = k_t c'_b$ (11)	$\left(\frac{d\theta}{dt}\right)_{i,d} = -\frac{k_t k_d \theta_i}{k_a (1-\theta_i)}$ (14)
reaction control ( $1-\theta \ll k_t$ )	$k_a \frac{d\theta}{dt} = k_a (1-\theta) (c'_b - c'_{eq})$ (9)	$\left(\frac{d\theta}{dt}\right)_{i,ads} = k_a c'_b$ (12)	$\left(\frac{d\theta}{dt}\right)_{i,d} = -k_d \theta_i$ (15)

10  
 11 \* Equations 5 and 7 are the general equations already indicated in the text, and equations 8 to 15 are derived from them  
 12 under special conditions of transport control, reaction control, initial adsorption or initial desorption, as indicated in the  
 13 table.

14 In all equations  $k_a$  is a constant for Langmuir kinetics and  $k_a = k_a^0 \exp(-b\theta)$  for FFG kinetics

15  $\Gamma_i, \theta_i$ : adsorbed amount and surface coverage at the beginning of the desorption experiment

16  $c'_{eq}$ : equilibrium concentration that corresponds to the specified  $\theta$

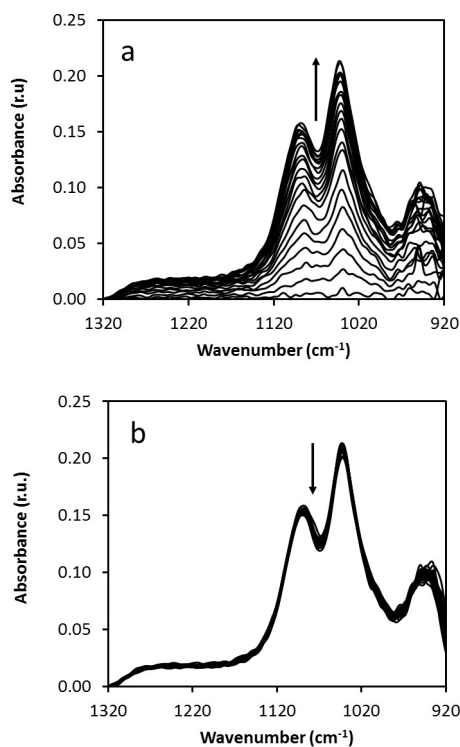
17  
 18

19 The equations written so far are rather general. By introducing the appropriate  
 20 definition of the rate coefficient  $k_a$ , for instance, the kinetic models related to Langmuir  
 21 or Frumkin-Fowler-Guggenheim (FFG) adsorption isotherms are obtained. If  $k_a$  is  
 22 considered to be a constant, independent on the surface coverage, eq. 6 is directly the  
 23 Langmuir isotherm, with  $\frac{k_a}{k_d} = K_L$ , the Langmuir constant. If on the contrary  $k_a$  is  
 24 considered to vary with the surface coverage as  $k_a = k_a^0 \exp(-b\theta)$ , eq. 6 becomes

$$\frac{\theta}{(1-\theta)} = \frac{k_a^o \exp(-b\theta)}{k_d} c'_{eq}$$

View Article Online  
DOI: 10.1039/D0CP00993H

- 2 Which is the FFG isotherm where  $k_a^o$  is a constant,  $\frac{k_a^o}{k_d} = K_{FFG}$  is the FFG constant and  $b$   
3 is the lateral interaction parameter (18).



- 4  
5 Fig. 2. ATR-FTIR spectra obtained during phosphate a) adsorption and b) desorption experiments. pH 7,  $c'_b$   
6  $=3 \times 10^{-6}$ . Arrows indicate increasing time.

## 8 Results and Discussion

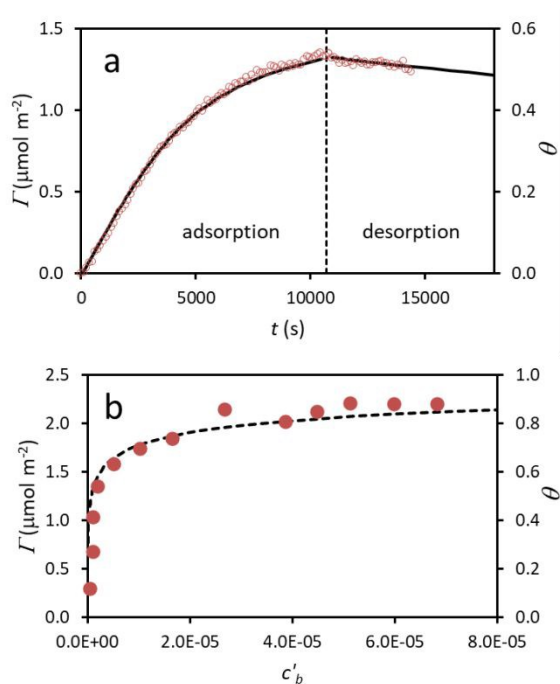
- 9 Figure 2 shows, as an example, the ATR-FTIR spectra obtained during adsorption-  
10 desorption kinetic measurements at pH 7.0 for a phosphate concentration  $3 \times 10^{-6}$  M ( $c'_b$   
11  $=3 \times 10^{-6}$ ). When the phosphate solution flowed in the system, the absorbance increased as  
12 time increased, indicating that adsorption was taking place. The reverse phenomenon,  
13 although less noticeable, was observed when the film was washed by flowing electrolyte  
14 at the same pH, indicating desorption. The spectra showed three main absorption bands,  
15 at 935, 1041 and 1091  $\text{cm}^{-1}$ , characteristic of an inner-sphere surface complex, the

1 monodentate mononuclear protonated species (9). The spectral shape did not change  
2 during adsorption and desorption, meaning that always the same species was present at  
3 the goethite surface. The behaviour shown in Fig. 2 for phosphate concentration  $c'_b=3\times 10^{-6}$   
4 was observed for all concentrations investigated. The only difference was in the  
5 adsorption rate, which increased by increasing  $c'_b$  (see below).

6 Figure 3a shows the  $\Gamma$  vs.  $t$  curve for the data corresponding to the adsorption-  
7 desorption experiment in Figure 2, whereas Figure 3b shows the phosphate adsorption  
8 isotherm.  $\Gamma$  vs.  $t$  curves were obtained by numerical integration (rectangle rule) of the  
9 general eq. 5, and the isotherm was calculated using eq. 16. In both figures experimental  
10 data (symbols) are compared to model calculations (lines, almost not seen because they  
11 are hidden by symbols) obtained with parameters listed in Table 2. This only set of  
12 parameters, as will be shown throughout this work, led to a very good simultaneous fit of  
13 the adsorption isotherm, the adsorption kinetics and the desorption kinetics, under all  
14 investigated conditions, giving confidence to the simple but very realistic model used  
15 here. The adsorption using  $c'_b=3\times 10^{-6}$  was relatively slow.  $\Gamma$  varied linearly with  $t$  in the  
16 initial part of the curve (Figure 3b), up to around 2000 s, corresponding to  $\Gamma$  values of  
17 around  $0.5 \mu\text{mol m}^{-2}$ . Many data points could be collected under this linear regime,  
18 guaranteeing a proper measurement of the initial adsorption rate from the initial slope of  
19  $\Gamma$  vs  $t$ . The desorption part of the curve also showed good linearity, with many data points,  
20 allowing also an appropriate measurement of the initial desorption rate. Even though  
21 reliable initial adsorption and desorption rates could be obtained under the working  
22 conditions, the meaning of these rates is vague without a clear visualization of the  
23 processes (transport, reaction, or both) controlling the adsorption.

24

25



View Article Online  
DOI: 10.1039/D0CP00993H

1  
2 Fig. 3. a) Adsorption-desorption kinetic curves for data in Fig. 2, pH 7,  $c'_b=3\times 10^{-6}$ . Symbols correspond to  
3 experimental points and lines correspond to model calculations (general equation 5/7, numerical  
4 integration, rectangle rule) with parameters from Table 2. b) Adsorption isotherm of phosphate on goethite  
5 at pH 7. Symbols correspond to experimental points and lines correspond to model calculations (FFG  
6 isotherm, equation 16) with parameters from Table 2.

7

8 **Table 2. Parameters of the model used in calculations\***

Parameter	
$k_a^0$ ( $\text{s}^{-1}$ )	$1.26\times 10^3$
$k_d$ ( $\text{s}^{-1}$ )	$1.66\times 10^{-5}$
$k_t$ ( $\text{s}^{-1}$ )	$3.54\times 10^1$
$b$	8.07
$\Gamma_m$ ( $\mu\text{mol m}^{-2}$ )	2.50

9 \* FFG kinetics was used in calculations with  $k_a = k_a^0 \exp(-b\theta)$

10

1           Figure 4 shows the experimental data obtained during adsorption experiments in  
2 terms of rate vs. adsorption curves ( $\frac{d\Gamma}{dt}$  vs.  $\Gamma$  curves). The rate was calculated from  
3 adsorption kinetic curves as  $\Delta\Gamma/\Delta t$  for each pair of adjacent data points, applying media  
4 average smoothing to avoid excessive scattering of data.  $\frac{d\Gamma}{dt}$  vs.  $\Gamma$  curves are very  
5 instructive because they allow analysing the progress of the rate as the surface is  
6 becoming populated by the adsorbed species and also permit the comparison of  
7 experimental rates with theoretical rates controlled either by transport or by reaction. Data  
8 in Figure 4 cover the full range of adsorption investigated, from  $c'_b=3\times 10^{-6}$  to  $c'_b=3\times 10^{-4}$ ,  
9 and very good fitting was obtained under all these conditions with the parameters of Table  
10 2. Figure 4a corresponds to the already analysed data in Figures 2 and 3. It is very clear  
11 for  $c'_b=3\times 10^{-6}$  that transport was much slower than attachment at the beginning of the  
12 reaction, and thus the process was transport-controlled at  $\Gamma < 0.5 \mu\text{mol m}^{-2}$ . Only when  $\Gamma$   
13 was relatively high ( $\Gamma > 1.2 \mu\text{mol m}^{-2}$ ), close to equilibrium values, the adsorption was  
14 reaction-controlled. Therefore, even though the initial adsorption rate could be properly  
15 measured, its value gives no information on rate coefficients  $k_a$  or  $k_d$ , because at the  
16 beginning the process is under transport control; only  $k_t$  could be obtained from the initial  
17 adsorption rate, with the use of eq. 11.

18           Figure 4 indicates that the adsorption became faster as the phosphate concentration  
19 increased. The initial adsorption rate was  $2.5\times 10^{-4} \mu\text{mol m}^{-2} \text{ s}^{-1}$  at  $c'_b=3\times 10^{-6}$ ,  $2.5\times 10^{-3}$   
20  $\mu\text{mol m}^{-2} \text{ s}^{-1}$  at  $c'_b=3\times 10^{-5}$  and around  $7.0\times 10^{-2} \mu\text{mol m}^{-2} \text{ s}^{-1}$  at  $c'_b=1\times 10^{-4}$ . At  $c'_b=3\times 10^{-4}$   
21 (Fig. 4d), which was the highest  $c'_b$  used, the adsorption was so fast that almost no data  
22 could be acquired at low  $\Gamma$  values and the initial adsorption rate could not be well  
23 measured. This is an important experimental disadvantage of relatively fast-adsorbing  
24 systems, where the scarcity of data makes very difficult to measure properly the initial  
25 adsorption rate under certain conditions. A second disadvantage of these fast systems is



1 that they easily become transport-controlled, as it occurs in all cases of Figure 4.  
2 Therefore, even assuming that the initial adsorption rate could be measured, the  
3 determination of the rate coefficients  $k_a$  and  $k_d$  is not possible.

4 Measuring and reporting adsorption rates is a very common practice in the  
5 literature and it is customary to extract rate coefficients from them (13)(19)(20)(21). As  
6 it can be seen with Figure 4, this practice can lead to misinterpretation of data if there is  
7 no information on whether transport or reaction is controlling the rate. The case analysed  
8 here, for example, corresponds to a relatively fast-adsorbing system, where the  
9 attachment is faster than transport. Therefore, besides resulting difficult to measure the  
10 adsorption rate under certain conditions, the process is normally controlled by transport,  
11 and thus attachment coefficients cannot be accessed from initial adsorption rates. The  
12 fitting of the full adsorption kinetic curve is needed for that purpose.

View Article Online  
DOI: 10.1039/C0CP00993H

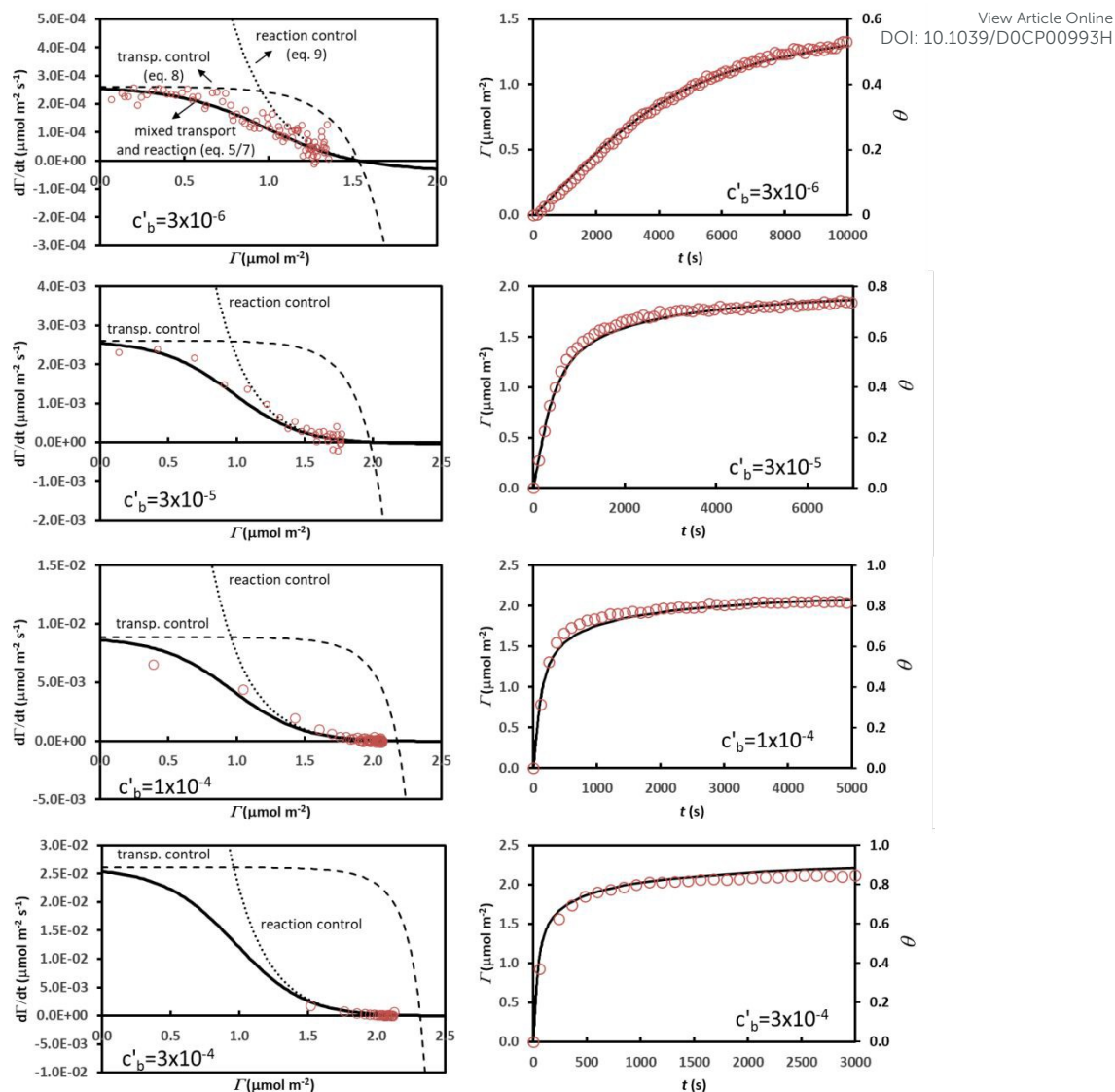
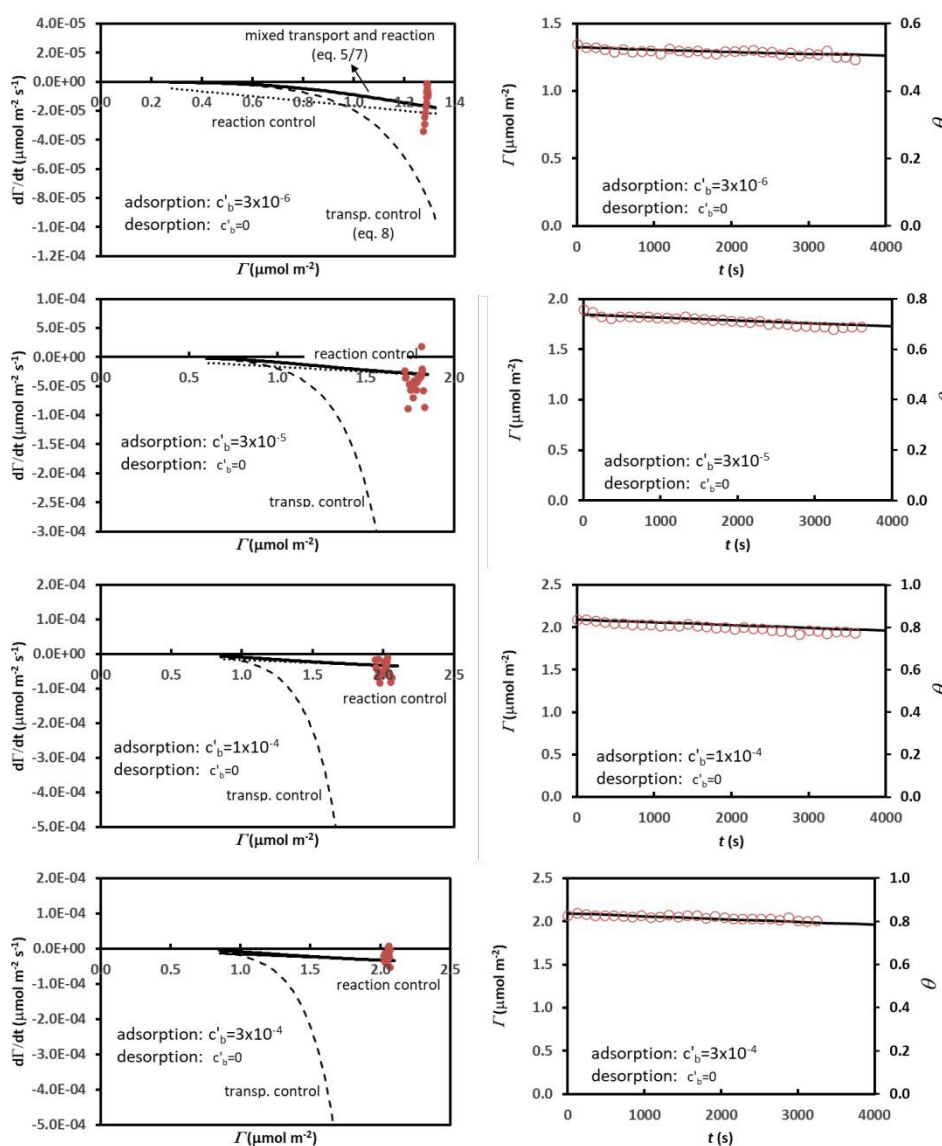


Fig. 4. Adsorption experiments. Rate vs  $\Gamma$  curves and adsorption kinetic curves for the investigated concentrations of phosphate. In all cases symbols correspond to experimental points and lines correspond to model calculations with parameters in Table 2.  $\Gamma$  vs.  $t$  curves were obtained by numerical integration (rectangle rule) of the general eq. 5.

Figure 5 shows the  $\frac{d\Gamma}{dt}$  vs.  $\Gamma$  and the  $\Gamma$  vs.  $t$  curves for desorption data. Experimental data are again compared to model calculations obtained with parameters listed in Table 2. Good linearity in the  $\Gamma$  vs.  $t$  curves was obtained, allowing for an appropriate determination of the initial desorption rates, which varied from  $-2 \times 10^{-5} \mu\text{mol m}^{-2} \text{s}^{-1}$  to  $-4 \times 10^{-5} \mu\text{mol m}^{-2} \text{s}^{-1}$  (negative values indicating desorption). This is a relatively slow-

1 desorbing system, the desorption process was always controlled by reaction (detachment)  
 2 as can be deduced from the comparison of experimental and theoretical rates in Figure 5.  
 3 It is so slow, that  $\Gamma$  decreased minimally in the time measured, and thus rate data could  
 4 be gathered for a small range of  $\Gamma$ , as can be seen in the left-hand side panels of Fig. 5. In  
 5 spite of this, the fact that desorption was reaction-controlled allowed for a very reliable  
 6 determination of  $k_d$  from the initial desorption rates (see Eq. 15). In combination with the  
 7 adsorption isotherm, it permits also to obtain  $k_a$  through the equilibrium adsorption  
 8 constant.



9

1 Fig. 5. Desorption experiments. Rate vs  $\Gamma$  curves and desorption kinetic curves for the investigated  
2 cases. The concentration used for adsorbing phosphate are indicated in the figure. In all cases desorption  
3 took place by flowing supporting electrolyte at pH 7 ( $c'_b=0$ ). Symbols correspond to experimental points  
4 and lines correspond to model calculations with parameters in Table 2.  $\Gamma$  vs.  $t$  curves were obtained by  
5 numerical integration (rectangle rule) of the general eq. 5.

6  
7 The value of the first-order desorption rate constant,  $k_d=1.66\times 10^{-5} \text{ s}^{-1}$ , indicates  
8 that the half-life of the desorption reaction ( $t_{1/2}=0.693/k_d$ ) is 41700 s (11.6 h), and that  
9 almost 40 h should be necessary to desorb 90% of the adsorbed phosphate. On the  
10 contrary, adsorption would take only a few seconds in absence of transport control. This  
11 is why an almost full adsorption curve can be obtained in a short time, even under  
12 transport control, as seen in the right-hand side panels of Fig. 4, but only the initial parts  
13 of the desorption curves can be registered in one hour (right-hand side panels of Fig. 5).

14 Desorption kinetic studies are completely neglected in the literature. However, for  
15 the phosphate-goethite system studied here, detachment is slower than transport and  
16 controls the rate. Consequently, desorption kinetics shows to be more important than  
17 adsorption kinetics for determining rate coefficients from initial rates. This could be the  
18 case for many environmentally and technologically relevant systems. The explanation of  
19 the observed behaviour comes from the fact that in adsorption-desorption the transport  
20 process is always connected in series to the reaction process, and thus the overall rate is  
21 dictated by the slowest process. The case of phosphate on goethite is a typical example  
22 where the high affinity of the ion for the surface results in a large  $k_a$  and a small  $k_d$ . This  
23 combination of rate constants leads to a fast adsorption, which becomes transport-  
24 controlled, and a slow desorption, which becomes reaction-controlled. Many adsorbing  
25 substances in the environment or industry, having high affinity for the solid surface, with  
26 large  $k_a$  and small  $k_d$ , may behave as phosphate on goethite. With all these fast-adsorbing

1 and slow-desorbing substances, measuring desorption kinetics is simpler and more  
2 informative than measuring adsorption kinetics.

3 It must be remarked that the measured adsorption and desorption rate constants  
4 are valid for the studied system at pH 7.0, which was the pH of the experiments. Changing  
5 pH changes the surface charge of the goethite surface and also may change the adsorbed  
6 species. For example, as indicated above, at pH 7.0 the phosphate species populating the  
7 goethite surface is a monoprotonated surface complex, whereas at low pH the prevailing  
8 species is a diprotonated surface complex (9). The rate constants at low pH are surely  
9 different because a different species is being adsorbed and desorbed. The methodology  
10 and model proposed here open the possibility of a realistic study of the very rich  
11 phosphate-goethite system, and many other systems where surface speciation changes by  
12 changing experimental conditions.

## 14 **Conclusions**

15 A simple, realistic and very effective model combining transport and reaction  
16 was successfully applied to describe simultaneously the adsorption-desorption kinetics at  
17 the solid/water interface as measured in an ATR-FTIR flow cell. The use of rate vs.  
18 adsorption curves ( $\frac{d\Gamma}{dt}$  vs.  $\Gamma$  curves) is enlightening because it permits to compare actual  
19 rates with theoretical rates controlled either by transport or reaction, and to define if the  
20 process is being transport- or reaction-controlled.

21 The model was able to describe the behavior of the phosphate-goethite system  
22 under a variety of conditions, and the adsorption kinetic runs, the desorption kinetic runs  
23 and adsorption isotherms could be reproduced using just one set of rate coefficients. Since  
24 phosphate had a high affinity for the goethite surface the chemical attachment was very  
25 fast, making adsorption to be transport-controlled, and the chemical detachment was very

1 slow, making desorption to be reaction-controlled. Therefore, obtaining reaction rate  
2 coefficients with this fast-adsorbing and slow-desorbing system was easier from  
3 desorption kinetic than from adsorption kinetic data.

4

## 5 Acknowledgments

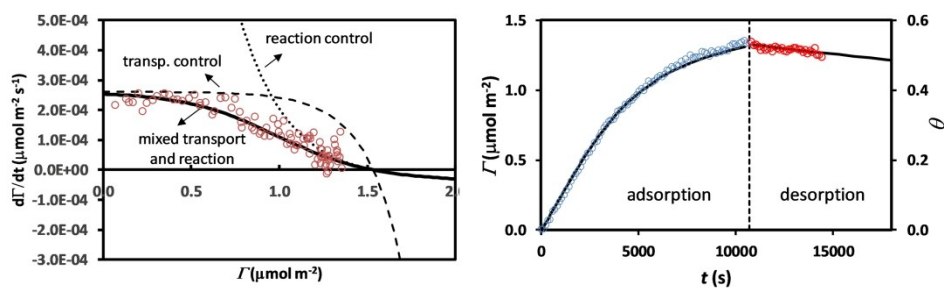
6 This work was financed by CONICET, FONCYT and SGCyT-UNS.

7

## 8 References

- 9 1. Sparks DL. Environmental Soil Chemistry: Second Edition. Environmental Soil  
10 Chemistry: Second Edition. Amsterdam: Academic Press; 2003. 352 p.
- 11 2. Norde W. Colloids and interfaces in life sciences and bionanotechnology: Second  
12 edition. Colloids and Interfaces in Life Sciences and Bionanotechnology: Second  
13 Edition. Boca Raton: CRC Press; 2011. 466 p.
- 14 3. Rahnemaie R, Hiemstra T, Van Riemsdijk WH. Geometry, charge distribution,  
15 and surface speciation of phosphate on goethite. *Langmuir*. 2007;23(7):3680–9.
- 16 4. Sverjensky DA. Interpretation and prediction of triple-layer model capacitances  
17 and the structure of the oxide-electrolyte-water interface. *Geochim Cosmochim*  
18 *Acta*. 2001;
- 19 5. Sparks DL. Kinetics of soil chemical processes. San Diego: Academic Press;  
20 1989. 210 p.
- 21 6. Regazzoni AE. Adsorption kinetics at solid/aqueous solution interfaces: On the  
22 boundaries of the pseudo-second order rate equation. *Colloids Surfaces A*  
23 *Physicochem Eng Asp*. 2020;585:124093.
- 24 7. Aguirre A, Berli CLA, Collins SE. ATR-FTIR spectrokinetic analysis of the CO  
25 adsorption and oxidation at water/platinum interface. *Catal Today*.  
26 2017;283:127–33.
- 27 8. Roncaroli F, Blesa MA. Kinetics of adsorption of oxalic acid on different  
28 titanium dioxide samples. *J Colloid Interface Sci*. 2011;356(1):227–33.
- 29 9. Arroyave JM, Puccia V, Zanini GP, Avena MJ. Surface speciation of phosphate  
30 on goethite as seen by InfraRed Surface Titrations (IRST). *Spectrochim Acta -*  
31 *Part A Mol Biomol Spectrosc*. 2018;199:57–64.
- 32 10. Sen Gupta S, Bhattacharyya KG. Kinetics of adsorption of metal ions on  
33 inorganic materials: A review. *Adv Colloid Interface Sci [Internet]*. 2011;162(1–  
34 2):39–58. Available from:  
35 <https://www.sciencedirect.com/science/article/pii/S0001868611000030>
- 36 11. Young AG, McQuillan AJ. Adsorption/Desorption Kinetics from ATR-IR  
37 Spectroscopy. Aqueous Oxalic Acid on Anatase TiO<sub>2</sub>. *Langmuir*.  
38 2009;25(6):3538–48.
- 39 12. Persson P, Nilsson N, Sjöberg S. Structure and bonding of orthophosphate ions at  
40 the iron oxide-aqueous interface. *J Colloid Interface Sci*. 1996;177(1):263–75.
- 41 13. Luengo C, Brigante M, Antelo J, Avena M. Kinetics of phosphate adsorption on  
42 goethite: Comparing batch adsorption and ATR-IR measurements. *J Colloid*

- 1 Interface Sci. 2006;300(2):511–8.
- 2 14. Kubicki JD, Paul KW, Kabalan L, Zhu Q, Mroziak MK, Aryanpour M, et al.
- 3 ATR-FTIR and density functional theory study of the structures, energetics, and
- 4 vibrational spectra of phosphate adsorbed onto goethite. *Langmuir*.
- 5 2012;28(41):14573–87.
- 6 15. Arroyave JM, Waiman CC, Zanini GP, Avena MJ. Effect of humic acid on the
- 7 adsorption/desorption behavior of glyphosate on goethite. Isotherms and kinetics.
- 8 *Chemosphere*. 2016;145:34–41.
- 9 16. Atkinson RJ, Posner AM, Quirk JP. Adsorption of potential-determining ions at
- 10 the ferric oxide-aqueous electrolyte interface. *J Phys Chem*. 1967;71(3):550–8.
- 11 17. Murphy J, Riley JP. A modified single solution method for the determination of
- 12 phosphate in natural waters. *Anal Chim Acta*. 1962;27(C):31–6.
- 13 18. Stumm W, Sigg L, Sulzberger B. *Chemistry of the solid-water interface :*
- 14 *processes at the mineral-water and particle-water interface in natural systems*.
- 15 New York: Wiley; 1992. 428 p.
- 16 19. Luengo C, Brigante M, Avena M. Adsorption kinetics of phosphate and arsenate
- 17 on goethite. A comparative study. *J Colloid Interface Sci*. 2007;311(2):354–60.
- 18 20. Johir MAH, Pradhan M, Loganathan P, Kandasamy J, Vigneswaran S. Phosphate
- 19 adsorption from wastewater using zirconium (IV) hydroxide: Kinetics,
- 20 thermodynamics and membrane filtration adsorption hybrid system studies. *J*
- 21 *Environ Manage*. 2016;167:167–74.
- 22 21. Xie F, Dai Z, Zhu Y, Li G, Li H, He Z, et al. Adsorption of phosphate by
- 23 sediments in a eutrophic lake: Isotherms, kinetics, thermodynamics and the
- 24 influence of dissolved organic matter. *Colloids Surfaces A Physicochem Eng*
- 25 *Asp*. 2019;562:16–25.
- 26



fast-adsorbing/slow desorbing systems: Easier to determine rate parameters from desorption kinetics

257x97mm (300 x 300 DPI)